

# Efficient Object Classification and Recognition in SAR Imagery

Ievgen M. Gorovyi and Dmytro S. Sharapov

Department of Microwave Electronics, Institute of Radio Astronomy of NAS of Ukraine  
4 Chervonopraporna Str., Kharkov 61002, Ukraine  
gorovoy@rian.kharkov.ua, sharapov@it-jim.com

**Abstract:** SAR is a very popular instrument for imaging of the ground surface. Possibility of high-resolution image formation makes it superior tool for various information extraction tasks. In the paper, a problem of automatic target recognition is comprehensively analyzed. An idea of azimuth and range target profiles fusion is proposed. It is demonstrated, that usage of a proper image preprocessing with appropriate feature extraction steps allow to achieve a competitive recognition accuracy while keeping a low-dimensionality of feature vectors. Experimental results are discussed for a publicly available MSTAR dataset.

**Keywords:** synthetic aperture radar; automatic target recognition; SAR image, feature extraction; support vector machines; object classification

## 1. Introduction

Synthetic aperture radar (SAR) is a widely used instrument for various remote sensing tasks [1]-[3]. Among them, the problem of automatic target recognition (ATR) has attracted a considerable attention of SAR research community [4]-[5].

It is known, that SAR images significantly differ from optical images [6]. Basically, two main challenges arise. Firstly, existence of the speckle noise due to a coherent acquisition of backscattered signals. Secondly, a varying reflectivity of man-made objects as a function of viewing angle. In this context, a multi-look processing has a great importance [1]-[3].

The problem is that the human visual system (HVS) often fails in real target identification. This explains a high interest in automatic methods for SAR ATR.

A typical SAR ATR problem can be divided into three key stages (Fig. 1).

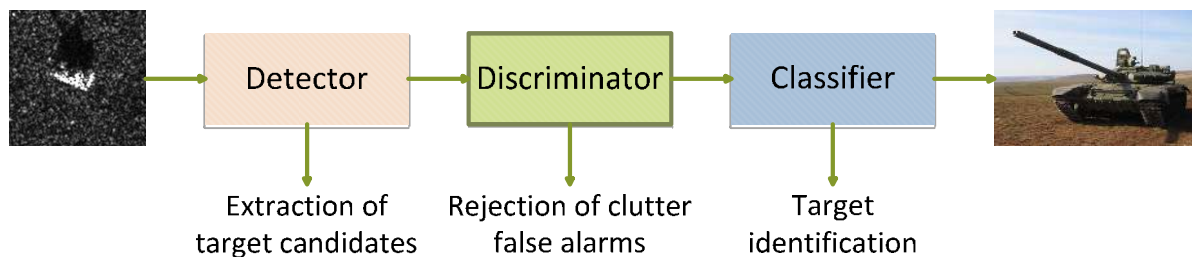


Figure 1. Key steps of ATR

The first stage is detection. Commonly, some target candidate regions are extracted from the initial SAR images [6]-[7]. Typically, there are a lot of false positives after this step. This can be easily explained due to the fact, that some clutter objects like buildings, trees, bridges also introduce high reflectivity level. This explains the necessity of the second step: discrimination. This stage can be considered as a two-class classification problem [6]-[7]. Finally, the third

step is target identification (recognition). A proper application of above three steps allows to detect and efficiently classify the objects of interest in SAR images.

Various approaches were used for SAR ATR problem. In [4] cepstrum coefficients features were extracted for automatic target recognition. Comparison with principal component analysis (PCA) and independent component analysis (ICA) has shown a good potential of such approach. In [5] PCA, ICA and Hu moment invariants were tested together with four different classifiers: linear discriminant classifier (LDC), quadratic discriminant classifier (QDC), k-nearest neighbors (k-NN) and support vector machines (SVM). Comparative experiments on 7 classes from moving and stationary target acquisition and recognition (MSTAR) database [5], [8] were conducted. In [9] Bayesian compressive sensing (BCS) technique was applied with scattering centers features. Comparative classification results for basis pursuit (BP), sparse representative classifier (SRC), SVM and BCS indicated on a high potential on the proposed technique.

The latest research results in pattern recognition indicated a great performance of convolutional neural networks (CNNs) for various pattern recognition tasks. However it was found [10] that direct application of CNN for ATR data leads to overfitting. This is caused by a limited amount of SAR images in the available real datasets. In order to handle this problem, it was proposed to use a new architecture based on sparsely connected layers. As a result, amount of parameters was substantially reduced and a very high recognition rate was achieved. Interesting, that separate CNN architectures can be used for both discrimination and classification steps.

A PCA-based technique called 2-D neighborhood virtual points discriminant embedding (2DPCA-based 2DNVPDE) was proposed in [11]. The advantage of the method is in possibility to achieve a high accuracy using low dimensional feature vectors.

High-resolution range profiles (HRRs) were successfully applied for identification of both static of moving targets [12]-[14].

In the paper, we consider several feature extraction procedures together with SVM classifier as a tool of choice. It is shown, that a high recognition accuracy for 10 classes of MSTAR database can be achieved with low dimensional and compact feature vectors. In particular, fusion of horizontal and vertical profiles allows to additionally improve the classification rate.

Section 2 contains a general information about object segmentation in MSTAR images. Several image features are considered. Real SAR data examples and experimental results are described in section 3.

## **2. SAR Image Processing and Feature Extraction**

### *A. SAR Object Segmentation*

Shape characteristics and geometric features are important for the target recognition performance [6]-[7]. Object segmentation is one of the possible ways of preprocessing. Let's consider how this step can be accomplished. Basically, there are three regions demonstrating different level of pixel brightness: target, shadow and clutter (Fig. 2). The intensities of target pixels are commonly the brightest ones, while the shadow pixels has the lowest amplitudes. The target part can be segmented using some basic steps: histogram equalization and thresholding with subsequent blob extraction. Shadow area can be easily localized as well (Fig. 2).

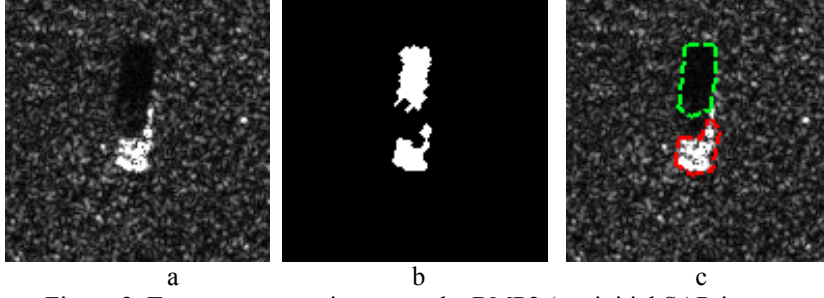


Figure 2. Target segmentation example, BMP2 (a – initial SAR image, b – extracted target and shadow blobs, c – SAR image with detected target and shadow)

One can see an example of SAR image of BMP2 from MSTAR database [8]-[9]. This dataset will be described in more detail in the experimental section of the paper. Binary image (Fig. 2b) illustrates an extracted target and shadow regions. Such localization steps can be accomplished in parallel. Finally, Fig. 2c illustrates the outlined target region of interest (ROI). Obviously, that geometrical features of target pixels area are changing with viewing angles and for different target categories. This should be accounted during feature extraction and classifications steps.

### B. Feature Extraction Procedure

Feature extraction is an important step in pattern recognition tasks. According to definition, features are numerical characteristics used for efficient and compact description of a particular visual object.

There are some common features which are typically used in object classification. In the paper, we are using Haralick features [15] and local binary patterns (LBP) [16] as a baseline features for comparison. The Haralick features are also known as a gray level co-occurrence matrices (GLCM) and widely used for the texture recognition tasks. For a given image  $I(x, y)$ , the co-occurrence matrix  $P$  is defined as

$$P_{ij} = \sum_{x=1}^N \sum_{y=1}^N \begin{cases} 1, & \text{if } I(x, y) = i \text{ and } I(x + \Delta_x, y + \Delta_y) = j, \\ 0, & \text{otherwise.} \end{cases} \quad (1)$$

where the offset  $(\Delta_x, \Delta_y)$  corresponds to the distance between the target pixel and corresponding neighbor.

As for LBP, the idea of the method is to generate a specific image from the initial image based on pixels comparison [16].

In the paper, we analyze a potential of range and azimuth profiles of the object of interest in SAR image. Such profiles can be calculated as

$$I_A^x = \frac{1}{NY} \sum_{y=1}^{NY} I(x, y), I_R^y = \frac{1}{NX} \sum_{x=1}^{NX} I(x, y), \quad (2)$$

where  $NX, NY$  are dimensions of image ROI. Fig. 3 illustrates an example of two images of T72 and single image BTR and corresponding image profiles. One can observe that range profiles for T72 target have a similar local pattern structure. In particular, sequences of local maxima and minima coincide. In contrast, corresponding range profile for BTR differs from the T72 profiles. As for the azimuth profiles, the distinction level is lower.

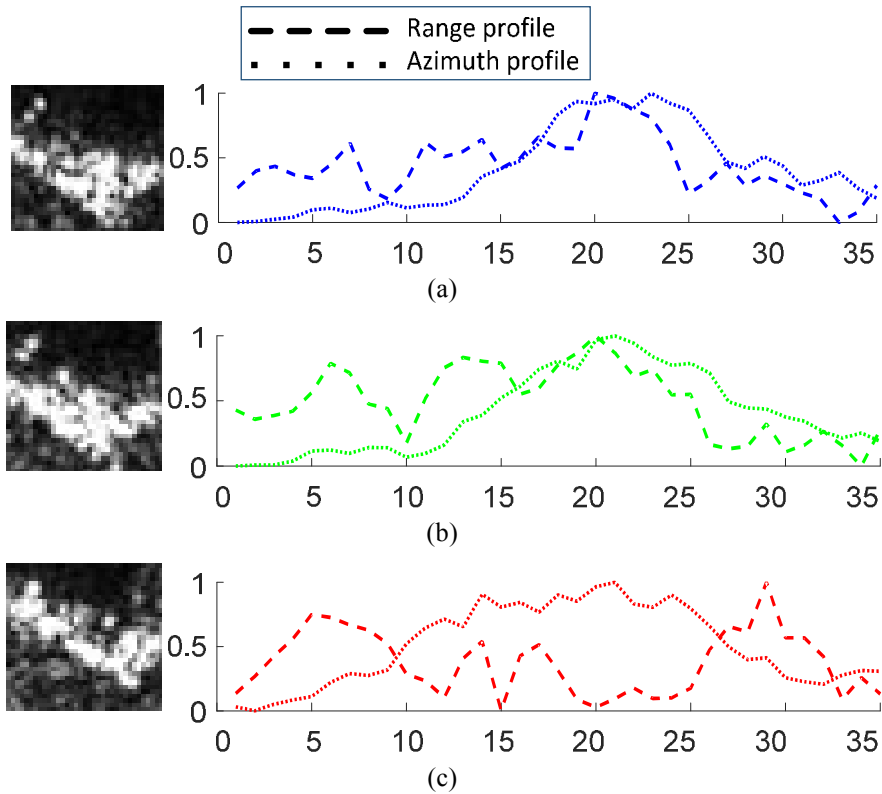


Figure 3. SAR images (MSTAR dataset, ROI size 35\*35) and profiles  
(a – T72 sample 1, b – T72 sample 2, c – BTR sample)

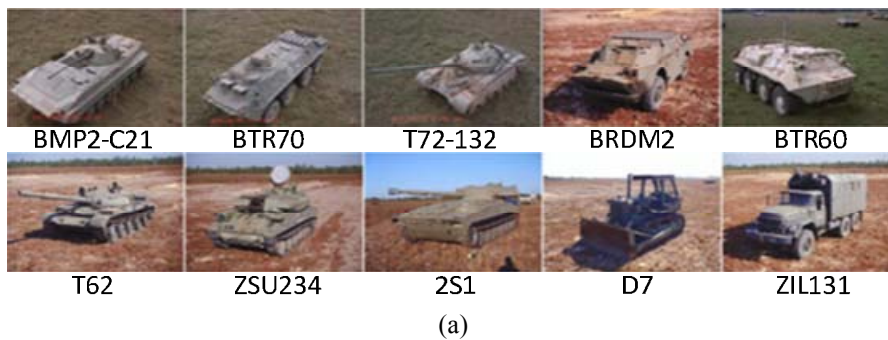
Classification results for the above described feature vectors types will be analyzed in the next section.

### 3. Real SAR Data and Recognition Results

This section contains a brief description of MSTAR database and obtained experimental results.

#### A. MSTAR Database

In our experiments, we have analyzed MSTAR dataset. It includes a series of 1 foot by 1 foot (0.3m by 0.3m) resolution spot-light mode SAR images which were collected using the Sandia National Laboratories by Twin Otter SAR sensor payload operating at X band. The images were taken over 360 degrees covering various target orientations. Fig. 4 illustrates optical and SAR images of corresponding military objects.



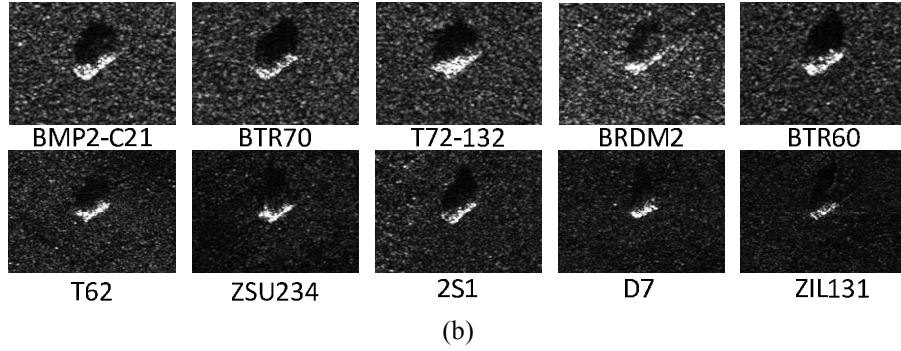


Figure 4. Images of 10 targets from MSTAR database  
(a – optical images, b – SAR images)

In particular, BMP2-C21, BTR70, T72-132, BRDM2, BTR60, T62, ZSU234, 2S1, D7, ZIL131. Apparently, that it is difficult to distinguish different targets in optical band by HVS (Fig. 4a). After comparison of images in optical and microwave bands (Fig. 4b), one can see that the target recognition problem is much more challenging for SAR imagery. Nevertheless, quite high accuracy was achieved during the tests. The next subsection contains the description of corresponding experimental results.

### B. Recognition Results

In order to compare the classification performance of different feature sets, we have trained the SVM classifier.

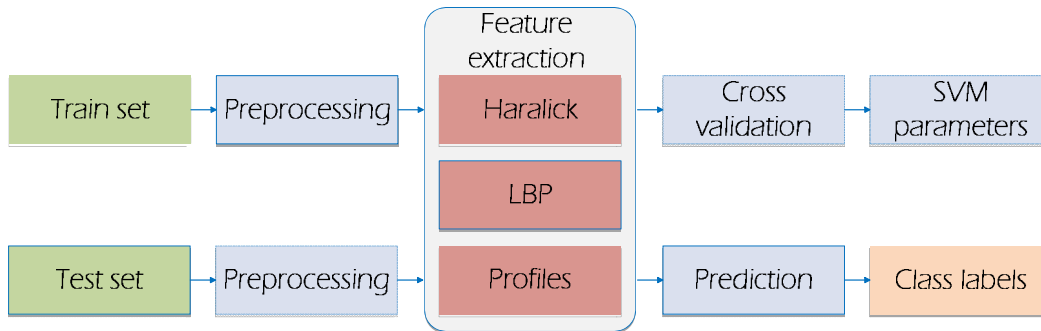


Figure 5. High-level diagram of SAR ATR algorithm

Fig. 5 contains a high-level diagram of SAR ATR algorithm. At the training stage, multiple local feature groups are extracted from the preprocessed SAR images. A cross-validation of SVM is performed for finding of optimal classifier parameters. As a result, classifier is ready for real data classification. At the testing stage, the trained model returns the predicted class labels for each calculated feature vector. We have used  $17^\circ$  depression angle images for the train set (3671 samples) and  $15^\circ$  depression angle (3203 samples) for the test set. Fig. 6 illustrates obtained recognition results for two sizes of SAR image ROI. One can observe that both Haralick and LBP features demonstrate quite low recognition rates. Azimuth profile features leads to only 58% of accuracy. However, fusion of range and azimuth profiles results in accuracy improvement from 81.5% to 90.7% for  $35 \times 60$  ROI size and from 77.1% to 81.4% for  $38 \times 35$  ROI size. One should emphasize that in the case of fusion of image profiles the length of feature vector is equal only to  $(N_{X_{ROI}} + N_{Y_{ROI}})$ , i.e. the sum of image dimensions. In contrast, Haralick feature vector is 195-dimensional, while LBP image feature vector is equal to  $(N_{X_{ROI}} \cdot N_{Y_{ROI}})$ .

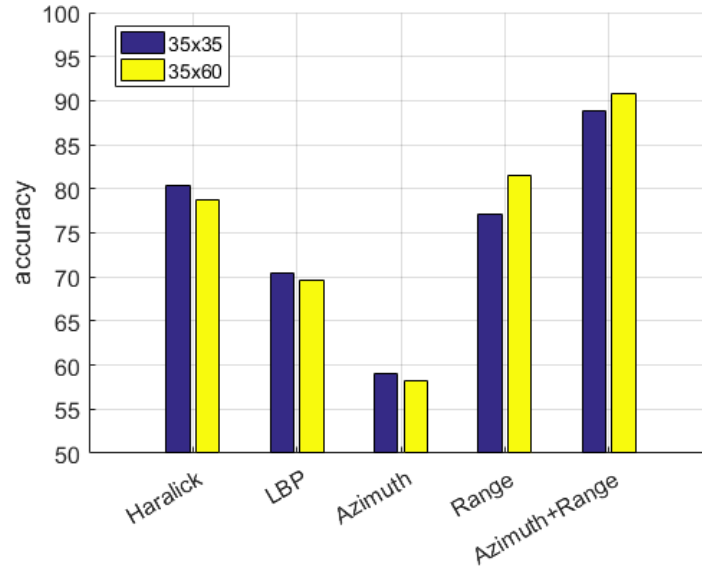


Figure 6. Accuracy for 10 classes recognition problem

Thus, proposed fused feature vector allows to obtain higher accuracy while keeping the low dimensionality.

In order to analyze the classification results in detail, the confusion matrix was built (Fig. 7).

predicted labels \ true labels	2S1	BRDM 2	BTR 60	D7	T62	ZIL131	ZSU 23 4	BMP2	BTR70	T72
2S1	0.92	0.00	0.00	0.01	0.00	0.01	0.03	0.02	0.00	0.00
BRDM 2	0.00	0.88	0.03	0.00	0.00	0.00	0.00	0.04	0.03	0.02
BTR 60	0.00	0.03	0.90	0.00	0.00	0.01	0.00	0.02	0.03	0.01
D7	0.02	0.00	0.00	0.83	0.07	0.07	0.00	0.00	0.00	0.00
T62	0.02	0.00	0.00	0.07	0.83	0.04	0.03	0.00	0.00	0.00
ZIL131	0.00	0.00	0.00	0.07	0.03	0.89	0.00	0.00	0.00	0.00
ZSU 23 4	0.02	0.00	0.00	0.00	0.01	0.00	0.97	0.00	0.00	0.00
BMP2	0.00	0.01	0.00	0.00	0.00	0.00	0.00	0.88	0.01	0.10
BTR70	0.00	0.02	0.00	0.00	0.00	0.00	0.01	0.05	0.91	0.02
T72	0.00	0.00	0.00	0.00	0.00	0.00	0.00	0.00	0.00	0.99

Figure 7. Confusion matrix for target recognition using profiles fusion

The average recognition accuracy is around 90.7%. One can see that for some classes (ZSU 234, T72) it is higher than for the rest of objects. Also, important information about false recognition is contained in the non-diagonal matrix elements. In particular, D7, T62 and ZIL 131 are problematic objects which demonstrate false classification for each other. In addition, 10% of T72 labels are predicted as BMP class. Such problems will be analyzed and solved in the near future.

#### 4. Conclusion

In the paper, the problem of SAR ATR was studied. Several feature types were analyzed and tested on real SAR dataset. Experimental analysis has shown that a proper extraction of image

ROI and construction of feature vectors allows to achieve competitive recognition results. Obtained accuracy indicates on a potential of the proposed classification scheme based on SAR ROI profiles fusion. In the near future, we are planning an additional improvement of the recognition rate and decreasing the feature vectors dimensionality at the same time. This will make possible to apply the developed solution on-board in real-time conditions.

## References

- [1] C. Oliver and S. Quegan, *Understanding Synthetic Aperture Radar Images*. Norwood, MA: Artech House, 1999.
- [2] G. Franceschetti and R. Lanari, *Synthetic Aperture Radar Processing*. CRC Press, 1999.
- [3] W. G. Carrara, R. S. Goodman, and R. M. Majewski, *Spotlight Synthetic Aperture Radar: Signal Processing Algorithms*. Boston; London: Artech House, 1995.
- [4] A. Eryildirim, *Methods for automatic target classification in radar*. Master thesis, Ankara, Bilkent University, 76 p, 2009.
- [5] J. Park and K.-T. Kim, "Modified polar mapping classifier for SAR automatic target recognition". *IEEE Transactions on Aerospace and Electronic Systems*, Vol. 50, No. 2, pp. 1092 – 1107, 2014.
- [6] D. Dugeon and R. Lacoss, "An overview of automatic target recognition". *Lincoln Laboratory Journal*, Vol. 6, No. 1, pp. 3–9, 1993.
- [7] L. Novak, G. Owirka and C. Netishen, "Performance of a high-resolution polarimetric SAR automatic target recognition system". *Lincoln Laboratory Journal*, Vol. 6, No. 1, pp. 11–24, 1997.
- [8] Y. Yang, Y. Qiu and C. Lu, "Automatic target classification experiments on the MSTAR SAR images". *Proceedings of the 6th International Conference on Software Engineering, Artificial Intelligence, Networking and Parallel/Distributed Computing and 1st ACIS International Workshop on Self-Assembling Wireless Networks*; pp. 2–7, 2005.
- [9] X. Z. Zhang, J. H. Qin, and G. J. Li, "SAR target classification using Bayesian compressive sensing with scattering centers features". *Progress in Electromagnetics Research*, vol. 136, pp. 385–407, 2013.
- [10] C. Sizhe; W. Haipeng; X. Feng and J. Ya-Qiu, "Target classification using the deep convolutional networks for SAR Images". *IEEE Transactions on Geoscience and Remote Sensing*, Vol. 54, No. 8, pp. 4806-4817, 2016.
- [11] J. Pei et al., "SAR imagery feature extraction using 2DPCA-Based two-dimensional neighborhood virtual points discriminant embedding". *IEEE Journal of Selected Topics in Applied Earth Observations & Remote Sensing*, Vol. 9, No. 6, pp. 2206-2214, 2016.
- [12] Wong, S. K., "High range resolution profiles as motion-invariant features for moving ground targets identification in SAR-based automatic target recognition". *IEEE Transactions on Aerospace and Electronic Systems*, Vol. 45, No. 3, 1512–1524, 2009.
- [13] S. Jacobs and J. O'Sullivan, "Automatic target recognition using sequences of high resolution radar range-profiles". *IEEE Transactions on Aerospace and Electronic Systems*, Vol. 36, No. 2, pp. 346–381, 2000.
- [14] R. Williams et al., "Automatic target recognition of time critical moving targets using 1D high range resolution (HRR) radar". *Radar IEEE Radar Conference*, pp. 37-44, 1999.
- [15] R. M. Haralick, "Statistical and structural approaches to texture". *Proc. IEEE*, Vol. 67, No. 5, pp. 786-804, 1969.
- [16] T. Ojala, M. Pietikainen and T. Maenpaa, "Multiresolution gray-scale and rotation invariant texture classification with local binary pattern". *IEEE Transactions on Pattern Analysis and Machine Intelligence*, Vol. 24, No. 7, pp. 971–987, 2002.